Nuclear Instruments and Methods in Physics Research B 392 (2017) 94–101

Contents lists available at ScienceDirect

Nuclear Instruments and Methods in Physics Research B

journal homepage: www.elsevier.com/locate/nimb

Charge-state related effects in sputtering of LiF by swift heavy ions

W. Assmann [a], B. Ban-d'Etat [b], M. Bender [c], P. Boduch [b], P.L. Grande [d], H. Lebius [b], D. Lelièvre [b], G.G. Marmitt [d], H. Rothard [b], T. Seidl [c], D. Severin [c], K.-O. Voss [c], M. Toulemonde [b,*], C. Trautmann [c,e]

[a] Ludwig-Maximilians-Universität München, 85748 Garching, Germany
[b] Centre de Recherche sur les Ions, les Matériaux et la photonique, CIMAP-GANIL, CEA–CNRS–ENSICAEN–Univ. Caen, 14070 Caen, France
[c] GSI Helmholtzzentrum für Schwerionenforschung, 64291 Darmstadt, Germany
[d] Univ. Fed. Rio Grande do Sul, BR-91501970 Porto Alegre, RS, Brazil
[e] Technische Universität Darmstadt, 64289 Darmstadt, Germany

ARTICLE INFO

Article history:
Received 5 January 2016
Received in revised form 2 December 2016
Accepted 5 December 2016
Available online 21 December 2016

Keywords:
Electronic energy loss
Sputtering
LiF
Jet component

ABSTRACT

Sputtering experiments with swift heavy ions in the electronic energy loss regime were performed by using the catcher technique in combination with elastic recoil detection analysis. The angular distribution of particles sputtered from the surface of LiF single crystals is composed of a jet-like peak superimposed on a broad isotropic distribution. By using incident ions of fixed energy but different charges states, the influence of the electronic energy loss on both components is probed. We find indications that isotropic sputtering originates from near-surface layers, whereas the jet component may be affected by contributions from depth up to about 150 nm.

1. Introduction

In many materials, the irradiation with swift heavy ions leads to sputtering at the surface [1] and defect creation in the bulk [2]. Both phenomena are directly linked to the large energy deposition by the ion projectiles via electronic excitation and ionization processes. Experimental on-line observation of the formation of defects in bulk material is difficult due to the short time scales of the energy deposition within a nanometric volume [3]. In contrast, sputtered atoms and molecules can act as probes because they are emitted within a time window of 10^{-13}–10^{-11} s even before the deposited energy is fully dissipated [4]. Sputtering experiments thus provide information on a time period when the atoms are still in motion.

The energy deposition of ionic projectiles depends on their velocity. For beam energies larger than a few ten keV/u electronic stopping prevails, i.e., the energy is primarily deposited to the target electrons. At lower beam energies, the energy loss is dominated by elastic collision processes with target atoms. Elastic collisions also exist at higher beam energies but their contribution strongly decreases with increasing beam velocity. Sputtering in the elastic collision regime results from individual atomic collisions [5,6] or from collision spikes [7]. The main parameter governing elastic sputtering is the sublimation energy of the target (see for example the determination of sputtering yield by the collision spike model for Pt and Au [1,6]). The small volume involved in the atomic process makes it possible to apply microscopic models and simulate the process, e.g., by molecular dynamics calculations [8], where the motion of each atom is followed in space and time. Such models help to identify suitable experiments to probe physical parameters relevant for sputtering. The situation is different in the electronic energy loss (S_e) regime, because it involves several steps on different time scales: (i) initial energy deposition to the electrons (10^{17}–10^{16} s), (ii) energy dissipation among the electrons (10^{16}–10^{14} s), and (iii) energy transfer to the atoms by electron-phonon coupling (10^{14}–10^{12} s) leading to atomic motion and finally damage of the atomic structure [9,10].

In contrast to elastic sputtering, electronic sputtering processes are much less intensively investigated. Theoretical descriptions of electronic sputtering effects are limited to few targets such as solid Ar [11,12], UO_2 [13] and LiF [14]. Experimental electronic sputtering yields were measured for several alkali and earth alkali halides and oxides such as SiO_2 [15], UO_2 [16,17], $Y_3Fe_5O_{12}$, $Gd_3Ga_5O_{12}$ [18], and a few others [1]. Among the ionic crystals, the largest data set is available for LiF with respect to track formation [19–21] as well as electronic sputtering [1,22]. Sputtering with swift heavy ions revealed a rather peculiar behavior including huge stoichiometric sputtering yields of the order of 10^4 and 10^5 atoms per incident ion and a power law dependence of the yield Y on the

* Corresponding author.
E-mail address: toulemonde@ganil.fr (M. Toulemonde).

http://dx.doi.org/10.1016/j.nimb.2016.12.013
0168-583X/

electronic energy loss ($Y \sim S_e^4$). Furthermore, the yield decreases with increasing angle of beam incidence according to $(\sin\alpha)^{-1.7}$, with α being the angle between beam and sample surface [1]. Most surprising is the angular distribution of the sputtered particles having two components, a broad isotropic distribution superimposed by a narrow jet-like peak that always appears normal to the sample surface, independent on the angle of beam incidence [1,22]. Angular distributions with a jet-like component were also observed for other ionic crystals (CaF_2, NaCl, etc), garnets such as $Y_3Fe_5O_{12}$ and $Gd_3Ga_5O_{12}$ [18], and UO_2 [16,17], however with smaller yields as compared to LiF [1,22]. The situation is even more complex when analyzing sputtered ions where the width of the angular distribution of positively charged Li(LiF)n clusters, e.g., is not necessarily jet-like but depends on the size of the sputtered clusters [23]. It is important to note that cluster emission contributes significantly to the secondary ion yield [23,24].

It was speculated that the jet component in LiF is associated to a pressure pulse [11,25–27] created along the ion path, whereas the isotropic component may be due to thermal evaporation from the surface [22]. An alternative interpretation is proposed by Cherednikov et al. [14] using simulations based on a hybrid scheme (treating the electrons within a three-dimensional electrostatic microscopic particle-in-cell scheme and the atomic motion by means of molecular dynamics). The calculations do not reproduce the huge sputtering yields but ascribe the jet component to the buildup of an electric field at the track surface that focuses negative ions towards the surface normal.

Here we present experiments where the charge state of the incoming ions was varied in order to test its influence on the yield and angular distribution and possibly provide information on the depth of origin of the sputtered particles [28]. LiF crystals were chosen as target because of the very large sputtering yield reported earlier [22]. It is known that the sputtering rate at a given beam energy is sensitive to the charge state of the ions because it directly scales with the electronic energy loss [29–32]. Ions of charge state below equilibrium (eq) charge state deposit smaller energy densities at the surface and thus produce lower sputtering yields than ions in equilibrium charge state (mean charge of equilibrium charge state distribution) as observed for Ti [33], vitreous SiO_2 [34], UF_4 [35], and WO_3 [36]. When entering into a target, projectiles with non-equilibrium (neq) charge state either lose electrons (charge < eq) or capture electrons (charge > eq). The stripping or capture length required to reach the equilibrium charge state depends on the ion velocity and the target components [37] and can be calculated using e.g. the CasP code [38,39]. Fig. 1 illustrates how the charge state and the respective energy loss of 1.1 MeV/u I ions (initial charge 12+) and of 3.5 MeV/u Pb ions (initial charge 39 +) changes along the trajectory in a LiF target. The stripping or capture of electrons proceeds until the ions reach the equilibrium charge state. For the given ions and energies, charge equilibrium occurs on a path length of ~20 nm and ~170 nm, respectively. We define this stripping equilibrium length as the distance where the ions reach 90% of the energy loss difference between non-equilibrium and equilibrium charge state.

In our experiment, the different stripping length of the two beams plays an important role because it allows us to test the influence of the electronic energy loss as a function of the depth in the target.

2. Experimental

Catcher-based sputtering experiments were performed at the electrostatic tandem accelerator (Garching, Germany) and at the GANIL cyclotron accelerator (Caen, France) using ions of eq and neq charge states. The tandem provided beams of $^{132}I^{12+}$ (1.1 MeV/u) and $^{197}Au^{15+}$ (1.0 MeV/u) ions. To achieve ions of

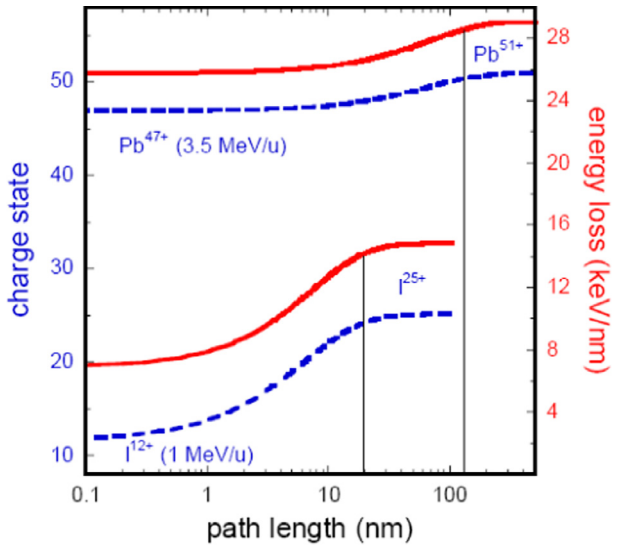

Fig. 1. Evolution of initial to equilibrium charge state (dashed blue lines) and corresponding electronic energy loss (solid red lines) along the ion path of Pb and I ions in LiF as function of the penetration depth. The equilibrium charge state is 25+ for ^{132}I at 1.1 MeV/u and 51+ for ^{208}Pb at 3.5 MeV/u [37]. Vertical lines denote the stripping length needed for the ions to reach 90% of the energy loss difference between non-equilibrium and equilibrium charge state. The stripping length is 19 nm for I ions and 170 nm for Pb ions. (For interpretation of the references to color in this figure legend, the reader is referred to the web version of this article.)

velocity-equivalent equilibrium charge states, a 10 μg/cm^2 thin carbon foil was mounted in front of the sputter target yielding a distribution of charge states around the respective equilibrium value of 25^+ for I and 31^+ for Au. At the GANIL accelerator, ^{208}Pb ions of 3.5 and 4.5 MeV/u were available. The charge states were varied by inserting a stripper foil in front of the magnetic beam selection system (alpha spectrometer) [40]. This provided charge state 23+ (below eq) and 56+ (eq) for 4.5 MeV/u Pb ions as well as 39+ (below eq), 47+ (below eq), 51+ (eq), and 55+ (above eq) for 3.5 MeV/u Pb ions.

To estimate the mean charge state of the projectiles along the ion path, rate equations [41] for the different charge-state fractions were solved by using adjustable electron-loss cross-sections from the CasP code [37–39] and capture cross-sections from the Bohr-Lindhard model [42] that reproduce the equilibrium charge-state values from Ref. [43–45]. The corresponding electronic energy loss shown in Fig. 1 was deduced by inserting the ion charge into the energy loss formula [37]. It is important to note that calculations based on codes such as CasP are needed because most energy loss codes including SRIM [46] assume equilibrium charge states and thus do not provide energy loss values for projectiles in non-equilibrium charge states. Comparing SRIM and CasP values for equilibrium charge states gives agreement within 10% for the ions used in our experiment. The stripping length of 3.5-MeV/u Pb ions of charge 23+, 39+, and 47+ is more than 130 nm, and the capture length for Pb^{55+} is close to 200 nm. Table 1 comprises the path length required to reach 90% of the electronic energy loss difference with respect to the equilibrium charge state. Fig. 2 shows the evolution of the charge state and electronic energy loss (S_e) as a function of the ion path in LiF for the different beams used as calculated by the CasP code [37]. The corresponding equilibration lengths are provided in Table 1.

Fig. 3 presents a photography of our sample set-up with the arc-shaped catcher mounted across the crystal. The experiments were performed for ion incidence angles of $\alpha = 20°, 30°$, and 70°. Sputtered atoms and molecules emitted from the target surface were collected on ultrapure Al catcher stripes mounted on the arc-shaped holder.